

See discussions, stats, and author profiles for this publication at: <https://www.researchgate.net/publication/234120646>

# Versatile Biofunctionalization of Polypeptide-Based Thermosensitive Hydrogels via Click Chemistry

ARTICLE in BIOMACROMOLECULES · JANUARY 2013

Impact Factor: 5.75 · DOI: 10.1021/bm3017059 · Source: PubMed

---

CITATIONS

20

---

READS

37

## 7 AUTHORS, INCLUDING:



**Yilong Cheng**

University of Washington Seattle

18 PUBLICATIONS 364 CITATIONS

[SEE PROFILE](#)



**Chunsheng Xiao**

Chinese Academy of Sciences

73 PUBLICATIONS 1,352 CITATIONS

[SEE PROFILE](#)



**Jianxun Ding**

Chinese Academy of Sciences

102 PUBLICATIONS 1,090 CITATIONS

[SEE PROFILE](#)



**Haitao Cui**

17 PUBLICATIONS 267 CITATIONS

[SEE PROFILE](#)

# Versatile Biofunctionalization of Polypeptide-Based Thermosensitive Hydrogels via Click Chemistry

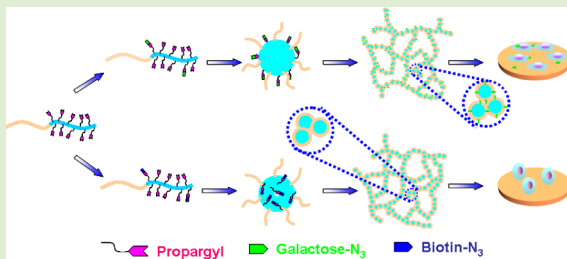
Yilong Cheng,<sup>†,‡</sup> Chaoliang He,<sup>†</sup> Chunsheng Xiao,<sup>†</sup> Jianxun Ding,<sup>†,‡</sup> Haitao Cui,<sup>†,‡</sup> Xiuli Zhuang,<sup>†</sup> and Xuesi Chen<sup>\*,†</sup>

<sup>†</sup>Key Laboratory of Polymer Ecomaterials, Changchun Institute of Applied Chemistry, Chinese Academy of Sciences, Changchun 130022, P. R. China

<sup>‡</sup>Graduate University of Chinese Academy of Sciences, Beijing 100039, P. R. China

## Supporting Information

**ABSTRACT:** In this study, we report thermosensitive hydrogels based on poly(ethylene glycol)-block-poly( $\gamma$ -propargyl-L-glutamate) (PEG-PPLG).  $^{13}\text{C}$  NMR spectra, DLS, and circular dichroism spectra were employed to study the mechanism of the sol–gel phase transition. Mouse fibroblast L929 cells were encapsulated and cultured within the hydrogel matrices, and the encapsulated cells were shown to be highly viable in the gel matrices, suggesting that the hydrogels have excellent cytocompatibilities. The mass loss of the hydrogels *in vitro* was accelerated by the presence of proteinase K compared to the control group. *In vivo* biocompatibility studies revealed that the *in situ* formed gels in the subcutaneous layer last for ~21 days, and H&E staining study suggested acceptable biocompatibility of our materials *in vivo*. The presence of alkynyl side groups in the PEG-PPLG copolymers allowed convenient further functionalization with azide-modified bioactive molecules, such as biotin and galactose. The biofunctionalized PEG–polypeptide block copolymers showed sol–gel phase transitions similar to the parent copolymers. Interestingly, the incorporation of galactose groups into the hydrogels was found to improve cell adhesion, likely due to the adsorption of fibronectin (FN) in cell–extracellular matrix (ECM). Because bioactive materials have shown unique advantages in biomedical applications, especially tissue engineering and regenerative medicine applications, we believe our novel functionalizable thermosensitive hydrogels have potential to serve as a versatile platform for the development of new biofunctional materials, for example, biahesive and bioresponsive hydrogels.



## INTRODUCTION

Thermoinduced *in situ* formed hydrogels have been intensively investigated for biomedical applications including sustained and localized delivery of drugs and biomolecules,<sup>1–3</sup> cell culture,<sup>4–6</sup> and tissue engineering.<sup>7–10</sup> For a typical thermogelling hydrogel system, polymer aqueous solutions with lower viscosity are obtained at lower temperatures, and the polymer solutions need to undergo spontaneous phase transition with increasing temperature to form physical gels. Hence, the polymer solution can be injected via minimally invasive administration and forms gels *in situ* to conform to the irregular shape of the treatment site. Moreover, this system also enables bioactive agents or cells to be easily mixed with the liquid precursor at lower temperature, and the bioactive agent or cell encapsulated hydrogels could be formed at the injection site to act as a sustained drug delivery depot or a three-dimensional matrix for cell proliferation or growth to a tissue.<sup>11–15</sup>

Thermosensitive biodegradable block copolymer hydrogels are one of the most studied injectable hydrogels, which are mainly composed of a hydrophilic poly(ethylene glycol) (PEG) block and a hydrophobic biodegradable block, such as poly(lactic acid) (PLA),<sup>16,17</sup> poly(lactic acid-*co*-glycolic acid) (PLGA),<sup>18,19</sup> poly( $\epsilon$ -caprolactone) (PCL),<sup>20</sup> poly( $\epsilon$ -caprolac-

tone-*co*-lactide) (PCLA),<sup>21</sup> poly((*R*)-3-hydroxybutyrate) (PHB),<sup>22</sup> poly(amidoamine) (PAA),<sup>23</sup> and polypeptides.<sup>24–27</sup> Very recently, hydrogels capable of displaying biological functions and responding to external biological stimuli have received increasing interest for their unique advantages in regenerative medicine, such as advantages in mimicking natural extracellular matrix (ECM) and regulating cell–material interactions. However, the usually high level of PEG segment on the surface of traditional block copolymer hydrogels has the tendency to be an impediment to both protein absorption and cell adhesion, making these materials relatively biological inert *in vivo*. In addition, due to the lack of functional groups on both the PEG and the hydrophobic segments, it has been a challenging task to fabricate functionalized thermogelling block copolymers.

In this work, poly(ethylene glycol)-block-poly( $\gamma$ -propargyl-L-glutamate) (PEG-PPLG) with pendent alkynyl groups was synthesized, and the resulting copolymer underwent sol–gel transition with changing temperature. Furthermore, the alkynyl groups could be functionalized with biomacromolecules

Received: November 5, 2012

Revised: January 10, 2013

Published: January 11, 2013



through click chemistry with high efficiency. The resulting block copolymer hydrogels exhibited good cytocompatibility *in vitro* and acceptable biocompatibility *in vivo*. Because the pendent alkynyl groups were present in the hydrophobic domains, and the water-solubility of the linked groups may affect not only the gelation behavior of the resulting copolymer, but also the bioactivity of the gel surface. The basic idea is schematically presented in Figure 1.

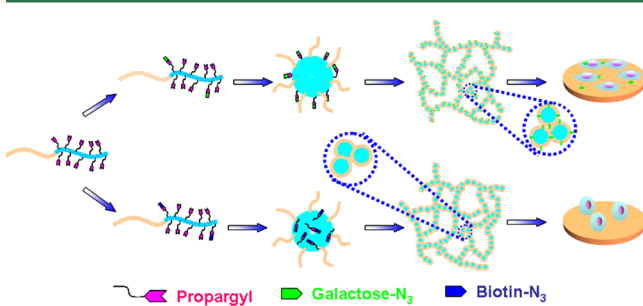


**Figure 1.** Schematic presentation of biofunctionalization of PEG-PPLG hydrogels with galactose and biotin. The effect of the linked molecules on cell adhesion was found to be different, which was attributed to the assemble pattern of the modified copolymers. The introduction of galactose promotes cell adhesion due to the exposure of galactose on the gel surface. In contrast, hydrogels functionalized biotin that is mostly restricted inside the micelles did not display significantly enhanced cell affinity.

As a proof-of-concept, we functionalized PEG-PPLG by using two bioactive molecules, galactose and biotin, to investigate the influence of the biofunctionalization on the phase transition and cell adhesion of the modified hydrogels. As a hydrophilic and water-soluble molecule, galactose can interact with some proteins, such as fibronectin (FN), an ECM component that plays a crucial role in mediating cell adhesion and therefore has potential in cell culture.<sup>28,29</sup> In aqueous solution, galactose may expose in the aqueous environment, which facilitates its interaction with other biomacromolecules and cells. The introduction of hydrophilic galactose may increase the phase transition temperature of the parent thermogelling block copolymers, due to the variation of hydrophilic/hydrophobic balance, and improve cell adhesion on the modified gel surface.

Biotin (vitamin H), one of the B complex vitamin families, is a growth promoter at the cellular level, which exists in liver, kidney, pancreas, and so on.<sup>30,31</sup> Its derivatives have been used in cancer therapy and tissue-engineering field.<sup>32,33</sup> In addition, biotin receptor is widely present in normal cells. Through the interaction between biotin and its receptor, the biotin-modified materials can enhance cell affinity or promote cells adhesion. On the other hand, because biotin is a relative hydrophobic molecule, it may tend to aggregate into the micelle core. Therefore, the movement of biotin after modification may be restricted in hydrophobic environment, which may lead to suppressed effect on cell adhesion compared to the hydrophilic bioactive molecule.

In the present work, we used rheometer to study the phase transition behavior of the functionalized copolymers, and it was expected that the results could give us the insight into the effect of the polarity of linked molecule on sol–gel transition. Meanwhile, mouse fibroblast L929 cells were used to examine cell adhesion behavior of the surface of various biofunctionalized hydrogels.

## EXPERIMENTAL SECTION

**Materials.** Monomethyl poly(ethylene glycol) (mPEG,  $M_n = 2000$ ) was purchased from Aldrich and used as received, and the amino group terminated poly(ethylene glycol) monomethyl ether (mPEG-NH<sub>2</sub>) was synthesized according to the literature procedure.<sup>34</sup>  $\gamma$ -Propargyl-L-glutamate N-carboxyanhydride (PLG NCA) was synthesized according to our previously reported method.<sup>35,36</sup> Azides of galactose and biotin were prepared similarly as described in the literature.<sup>35,37</sup> THF was refluxed with sodium and distilled under nitrogen prior to use. *N,N*-Dimethylformamide (DMF) was stored over calcium hydride (CaH<sub>2</sub>) and purified by vacuum distillation. All the other reagents and solvents were purchased from Sinopharm Chemical Reagent Co. Ltd., China, and used as obtained.

**Characterization.** Proton nuclear magnetic resonance (<sup>1</sup>H NMR) spectra of poly(ethylene glycol)-block-poly( $\gamma$ -propargyl-L-glutamate) in trifluoroacetic acid-*d* (TFA-*d*) was recorded on a Bruker AV 400 NMR spectrometer. <sup>13</sup>C NMR spectral changes of PEG<sub>45</sub>-PPLG<sub>10</sub> (12.0 wt % in D<sub>2</sub>O) were investigated as a function of temperature in the range of 20–60 °C, and the solution temperature was equilibrated for 20 min before measurement. ATR-FTIR spectra were recorded for 12.0 wt % polymer solutions in D<sub>2</sub>O. The internal reflection element was a zinc selenide ATR plate. To analyze their secondary structure, deconvolution of the FTIR spectra was performed in the amide I band region of 1600–1700 cm<sup>-1</sup>. The deconvoluted spectra were fitted with Gaussian–Lorentzian sum function (20% Gaussian and 80% Lorentzian) using XPSPEAK software 4.1. The weight-average molecular weights ( $M_w$ ) and molecular distributions (polydispersity index, PDI =  $M_w/M_n$ ) were determined by gel permeation chromatography (GPC) using a series of liner Tskgel Super columns (AW3000 and AW5000) and Waters 515 HPLC pump with OPTILAB DSP interferometric refractometer (Wyatt Technology) as the detector. The eluent was DMF containing 0.01 M LiBr at a flow rate of 1.0 mL min<sup>-1</sup> at 50 °C. Monodispersed polystyrene standards purchased from Waters with a molecular weight range of 1790 to 2.0 × 10<sup>5</sup> were used to generate the calibration curve. The ellipticity of polymer aqueous solution (0.01 g L<sup>-1</sup>) was obtained on a JASCO J-810 spectrometer as a function of temperature in the range of 10–60 °C. TEM measurement was performed on a JEOL JEM-1011 transmission electron microscope with an accelerating voltage of 100 KV. A drop of polypeptides aqueous solution (0.50 g L<sup>-1</sup>) was deposited onto a 230 mesh copper grid coated with carbon and allowed to dry at room temperature before measurement. DLS measurements were performed on a WyattQELS instrument with a vertically polarized He–Ne laser (DAWN EOS, Wyatt Technology) and 90° collected optics. The sample was prepared in aqueous solution at a concentration of 1.0 wt %. Before measurements, the solution was filtered through a 0.45 μm Millipore filter. Fluorescence excitation spectra were recorded on a Perkin-Elmer LS50B luminescence spectrometer at the detection wavelength ( $\lambda_{em}$ ) of 390 nm.

**Synthesis of PEG-PPLG.** The block copolymers were synthesized by ring-opening polymerization (ROP) of  $\gamma$ -propargyl-L-glutamate N-carboxyanhydride (PLG NCA) in the presence of amino-terminated mPEG (denoted as mPEG<sub>45</sub>-NH<sub>2</sub>). A typical procedure for the preparation of PEG<sub>45</sub>-PPLG<sub>10</sub> was briefly as follows: mPEG<sub>45</sub>-NH<sub>2</sub> (1.0 g, 0.5 mmol) was dissolved in toluene (20.0 mL) and the residual water was removed by azeotropic distillation. Anhydrous *N,N*-dimethylformamide (DMF, 20.0 mL) and PLG NCA (1.266 g, 6.0 mmol) were added to the dried mPEG<sub>45</sub>-NH<sub>2</sub>. The reaction mixture was stirred at 25 °C for 3 days under a dry nitrogen atmosphere. Then the copolymer was purified by precipitation into glacial diethyl ether and filtered. The obtained product was further washed twice with diethyl ether and dried under vacuum. The yield was ~65%. Other copolymers with different degrees of polymerization (DP) were similarly prepared, and the compositions of the resulting copolymers are listed in Table 1.

**Synthesis of Biotin and Galactose Functionalized Copolymers.** The modified copolymers were synthesized by click chemistry. A typical procedure for the preparation of biotin functionalized PEG-PPLG (P-Biotin) was briefly described as follows: PEG<sub>45</sub>-PPLG<sub>10</sub>

**Table 1. Characterizations of the Block Copolymers**

code	DP of PPLG <sup>a</sup>	$M_n^a$	$M_w^b$	PDI <sup>b</sup>	CMC ( $10^{-3}$ /g L <sup>-1</sup> )
P1(PEG <sub>45</sub> -PPLG <sub>6</sub> )	6	3000	6900	1.10	8.53
P2(PEG <sub>45</sub> -PPLG <sub>10</sub> )	10	3700	7800	1.19	3.64
P3(PEG <sub>45</sub> -PPLG <sub>15</sub> )	15	4500	10700	1.16	1.02

<sup>a</sup>Determined by <sup>1</sup>H NMR. <sup>b</sup>Determined by GPC.

(1.28 g, 0.35 mmol) and biotin-N<sub>3</sub> (0.23 g, 0.69 mmol) were dissolved in 20.0 mL of DMSO, then the mixture was bubbled with nitrogen for 30 min. CuSO<sub>4</sub>·SH<sub>2</sub>O (0.035 g) was then introduced into the mixture under nitrogen bubbling for 5 min followed by sodium ascorbate (NaAsc, 0.14 g) addition. The flask was sealed under nitrogen and immersed in an oil bath at 40 °C for 3 days. The reaction was stopped by adding a small amount of deionized water. DOWEXHCRW2 resins (450 mg) were added and the mixture was stirred overnight to remove copper ions. After filtration, the solution was dialyzed against deionized water for 3 days using a dialysis bag (MWCO 3500 Da). The final product was obtained by lyophilization, and the yield was ~74%. Galactose functionalized PEG-PPLG (P-Gal) was prepared with the same procedure, and the yield was ~68%.

**Phase Diagram.** The sol–gel transition behavior of the polymer phosphate buffered saline (PBS, pH 7.4) solution was determined by the inverting test tube method with a temperature increment of 1 °C per step. Each sample at a given concentration was dissolved in PBS and stirred at 0 °C for 24 h. The copolymer PBS solution (0.5 mL) was introduced to the test tube with an inner diameter of 11 mm. The system was regarded as a gel in the case of no flow within 30 s.

**Dynamic Mechanical Analysis.** Rheology experiments were performed on a US 302 rheometer (Anton Paar). The copolymer solution was placed between parallel plates of 25 mm diameter and a gap of 0.5 mm. To prevent the evaporation of water, a layer of oil was put around the copolymer samples. The data were collected under a controlled strain γ 1% and a frequency of 1 rad s<sup>-1</sup>. The heating rate is 0.5 °C min<sup>-1</sup>.

**Cell Studies.** Mouse fibroblast L929 cells were cultured in complete Dulbecco's modified Eagle's medium (DMEM) containing 10% fetal bovine serum, supplemented with 50 IU mL<sup>-1</sup> penicillin and 50 IU mL<sup>-1</sup> streptomycin, and incubated at 37 °C in 5% CO<sub>2</sub> atmosphere. After sterilization by UV irradiation for 30 min at 0 °C, the PEG<sub>45</sub>-PPLG<sub>10</sub> PBS solutions (12.0 wt %, 0.2 mL) were mixed with harvested cells (5 × 10<sup>4</sup> cells) at 15 °C and maintained at 37 °C for 20 min in 24-well culture plates to form cell-encapsulating hydrogels. DMEM (0.5 mL) was added on the top of the cell-laden hydrogels and the medium was replaced every 2 days by a fresh medium. The viability of L929 cells with the hydrogels was determined using a Live/Dead kit. After the determined time intervals, culture medium was removed, and the hydrogels were washed three times with PBS. Afterward, cells encapsulated in the hydrogels were

incubated in a solution of 4.0 μM propidium iodine (PI) and 2.0 μM calcein AM in PBS. Viable cells were stained with calcein AM (green), and dead cells were stained with PI (red).

For the cell adhesion study, L929 cells suspended in complete DMEM containing FBS were seeded onto gel sheets prepared in 24-well culture plates at 2.0 × 10<sup>4</sup> cells well<sup>-1</sup> to study the adhesion of cells at 24 h. TCP without hydrogels was set as positive control. After the predetermined period, the incubation medium was removed and the plates were washed with PBS for three times. In addition, cell counting kit-8 (CCK-8) solution (1.0 mL; 10%, v/v in medium) was added to each well. After 4 h of incubation, the absorbance value at 450 nm was measured with an ELISA reader (Model 550; Bio-Rad, Hercules, CA, U.S.A.). Absorbance at 600 nm was used for baseline correction.

The relative cytotoxicities of the modified copolymers were assessed by methyl thiazolyl tetrazolium (MTT) viability assay against L929 cells. The cells were seeded in 96-well plates at 10000 cells per well in 200 μL of complete Dulbecco's modified Eagle's medium (DMEM) containing 10% fetal bovine serum, supplemented with 50 U/mL penicillin and 50 U/mL streptomycin, and incubated at 37 °C in 5% CO<sub>2</sub> atmosphere for 24 h, followed by adding copolymer solutions (20 μL in complete DMEM medium) at different concentrations (0.03–2.0 g L<sup>-1</sup>). The cells were subjected to MTT assay after being incubated for another 24 h. The absorbance of the solution was measured on a Bio-Rad 680 microplate reader at 492 nm. Cell viability (%) was calculated according to the following equation:

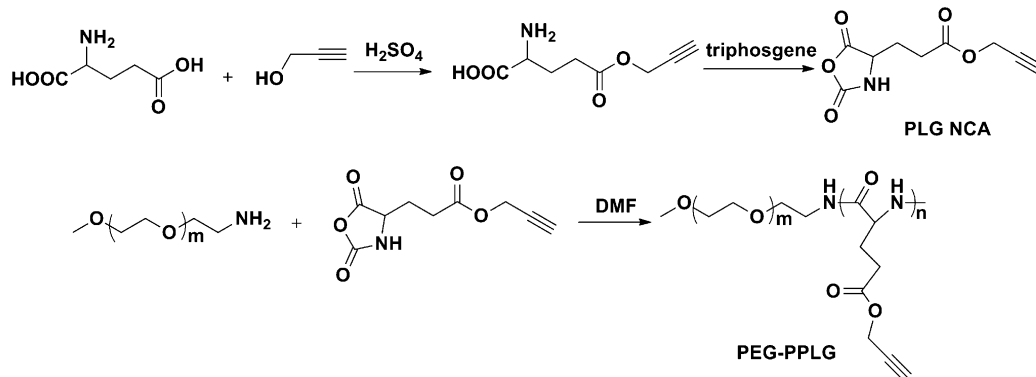
$$\text{cell viability}(\%) = (A_{\text{sample}}/A_{\text{control}}) \times 100\%$$

where  $A_{\text{sample}}$  and  $A_{\text{control}}$  were the absorbances of the sample and control well, respectively. The measurements were performed in triplicate.

**In Vitro Gel Duration.** The PEG-PPLG hydrogels were obtained by incubating 0.5 mL copolymer solutions in PBS (12.0 wt %) within different vials (diameter = 16 mm) at 37 °C for 10 min. Tris-HCl buffer solution (0.05 M, pH 7.4) containing 0.2 mg mL<sup>-1</sup> proteinase K, 10.0 mM CaCl<sub>2</sub>, and 0.2 wt % NaNO<sub>3</sub> was used as the degradation medium, and hydrogels incubated in Tris-HCl buffer solutions were used as the control. The buffer solution (3.0 mL) was added on the top of the gels at 37 °C and the whole medium was replaced every day. The mass of the remaining gel was measured at different time intervals.

**In Vivo Gel Degradation and Biocompatibility.** Sprague–Dawley (SD) rats (~200 g) were used for the in vivo testing. Rats were anesthetized by inhalation of diethyl ether, and 0.5 mL of PEG<sub>45</sub>-PPLG<sub>10</sub> PBS solution (12.0 wt %) was subcutaneously injected into dorsal areas of rats with a 21-gauge needle. At predetermined intervals, rats were sacrificed for the photographs collection. The tissues around the injection sites were surgically removed and histologically processed using hematoxylin-eosin stains for evaluation of inflammatory responses of the block copolymer in rats.

**Animal Procedure.** The animal experiments were carried out according to the guide for the care and use of laboratory animals,

**Scheme 1. Synthetic Route of Poly(ethylene glycol)-block-poly( $\gamma$ -propargyl-L-glutamate) (PEG-PPLG)**

provided by Jilin University, Changchun, China, and the procedure was approved by the local Animal Ethics Committee.

**Statistical Analysis.** Independent experiments were performed at least three times and triplicate samples were analyzed in each experiment. The significance of data obtained with the control and treated groups was statistically analyzed using the paired Student's *t*-test.

## RESULTS AND DISCUSSION

As shown in Scheme 1, PEG-PPLG was synthesized through the ROP of PLG NCA with mPEG-NH<sub>2</sub> as macroinitiator. The structures of the resulting copolymers were determined by <sup>1</sup>H NMR and GPC. The typical <sup>1</sup>H NMR spectra of PEG<sub>45</sub>-PPLG<sub>10</sub> in trifluoroacetic acid-*d* (TFA-*d*) is shown in Figure 2A, and all peaks have been well assigned. There was a sharp

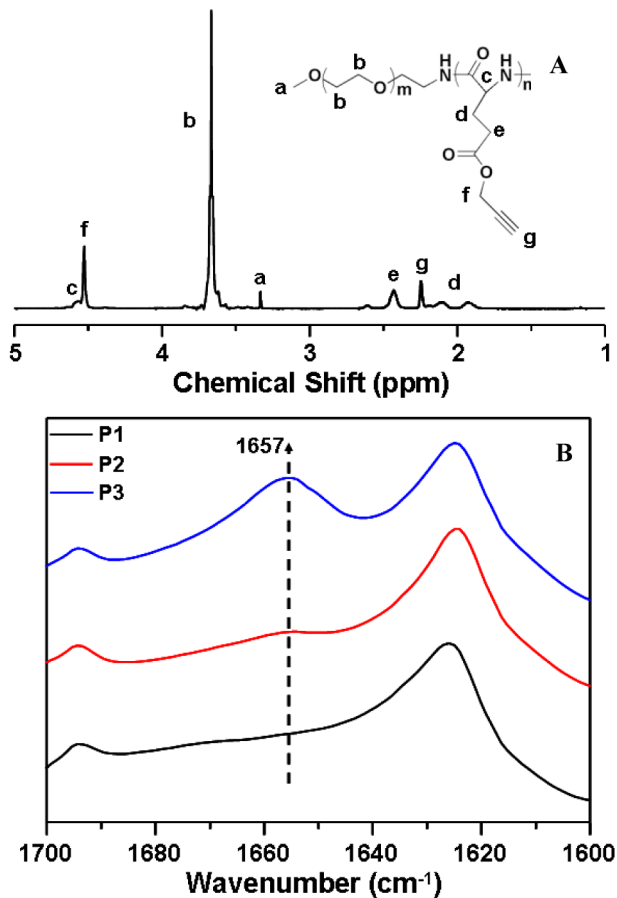


Figure 2. (A) <sup>1</sup>H NMR spectra of PEG-PPLG in TFA-*d*. (B) FTIR spectra of copolymers in the solid state.

peak at 2.5 ppm, suggesting the successful introduction of alkynyl group. The DP of the polypeptide backbone was calculated by comparing the integration of the methylene peak of poly(ethylene glycol) ( $-\text{CH}_2\text{CH}_2\text{O}-$ ) with that of the methylene peak of the glutamate units ( $-\text{CH}_2\text{CH}_2\text{C}(\text{O})-$ ). As summarized in Table 1, copolymers with DP ranging from 6 to 15 were prepared. The polydispersities (PDIs) determined by GPC were in the range of 1.1–1.2, indicating that the copolymers were all well prepared.

To investigate the secondary structure of the resulting copolymers, FTIR spectra were performed in solid state. As shown in Figure 2B, a sharp absorption band at 1627 cm<sup>-1</sup> was observed, which indicated that all copolymers adopted

predominantly  $\beta$ -sheet conformation.<sup>35</sup> On the other hand, the absorption band at 1657 cm<sup>-1</sup>, suggesting  $\alpha$ -helical conformation, increased when the molecular weight of the polypeptide block increased from 1000 to 2500 Da.<sup>36</sup> It demonstrated that the higher DP promoted the secondary conformation transition from  $\beta$ -sheet to  $\alpha$ -helix.<sup>38,39</sup> Meanwhile, ATR-FTIR was used to analyze the amide I band at 1600–1700 cm<sup>-1</sup> to study the secondary structure in solution state.<sup>40</sup> The results are listed in Table 2 and deconvolution of

Table 2. Percentage Content of Secondary Structures of the Polypeptides

code	helix (%)	$\beta$ -sheet (%)	random coil (%)	others (%)
P1	10	80	4	6
P2	15	74	6	5
P3	31	56	8	5

amide I band in FTIR spectra of P2 (12.0 wt % in D<sub>2</sub>O) is shown in Figure S1, in Supporting Information. As the DP of the polypeptide block increased from 6 to 15, the content of  $\beta$ -sheet decreased from 80 to 56%, while the  $\alpha$ -helix content increased from 10 to 31%.

In aqueous solution, the resulting copolymers were found to self-assemble into micelles. The typical micrograph of PEG<sub>45</sub>-PPLG<sub>10</sub> micelles is shown in Figure S2A, which take a spherical shape with a diameter of about 30 nm. Furthermore, we investigated their critical micelle concentrations (CMC) by the pyrene-probe-based fluorescence technique.<sup>41,42</sup> The excitation spectra of pyrene as a function of the concentration of the copolymers were measured. Figure S2B shows the fluorescence excitation spectra of pyrene in the PEG<sub>45</sub>-PPLG<sub>10</sub> solutions with different polymer concentrations. A red shift of (0, 0) absorption band from 332 to 336 nm was observed when the concentration of the copolymer increased from  $1.39 \times 10^{-4}$  to  $5.70 \times 10^{-1}$  g L<sup>-1</sup>. This red shift was resulted from the transfer of pyrene molecules from aqueous environment to the hydrophobic core, indicating the formation of micelle. In addition, CMC values were obtained from the plot of fluorescence intensity ratio of  $I_{336}/I_{332}$  versus  $\log_{10}c$  of the copolymers (Figure S2C). As listed in Table 1, their CMC values decreased from  $8.52 \times 10^{-3}$  to  $1.02 \times 10^{-3}$  g L<sup>-1</sup> as the molecular weight increased.

The PBS solution of the copolymers underwent sol–gel transition with increasing temperature. Hence, the widely used test tube inverting method was performed to study the transition temperature.<sup>43</sup> The sample is regarded as a gel if no flow was observed within 30 s after the vial was inverted. The phase diagrams of these block copolymers are shown in Figure 3A. All the copolymers underwent sol–gel transitions. It was found that an increase in the polypeptide block length resulted in a decline in sol–gel transition temperature, probably due to the increase in hydrophobic interactions among the polypeptide blocks.<sup>44</sup> For the rheology test (Figure 3B), the  $G'$  of PEG<sub>45</sub>-PPLG<sub>10</sub> solution was lower than  $G''$  in the low temperature range, exhibiting a typical liquid state. On the other hand, a significant increase in  $G'$  was observed with increasing temperature, while the increase in  $G''$  was relatively slow, which indicated the gel formation. The transition temperature obtained from the marked increase of  $G'$  coincided well with that determined by test tube inverting method. In addition, we also investigated the change of storage modulus with the variation of copolymer concentration. An increase in

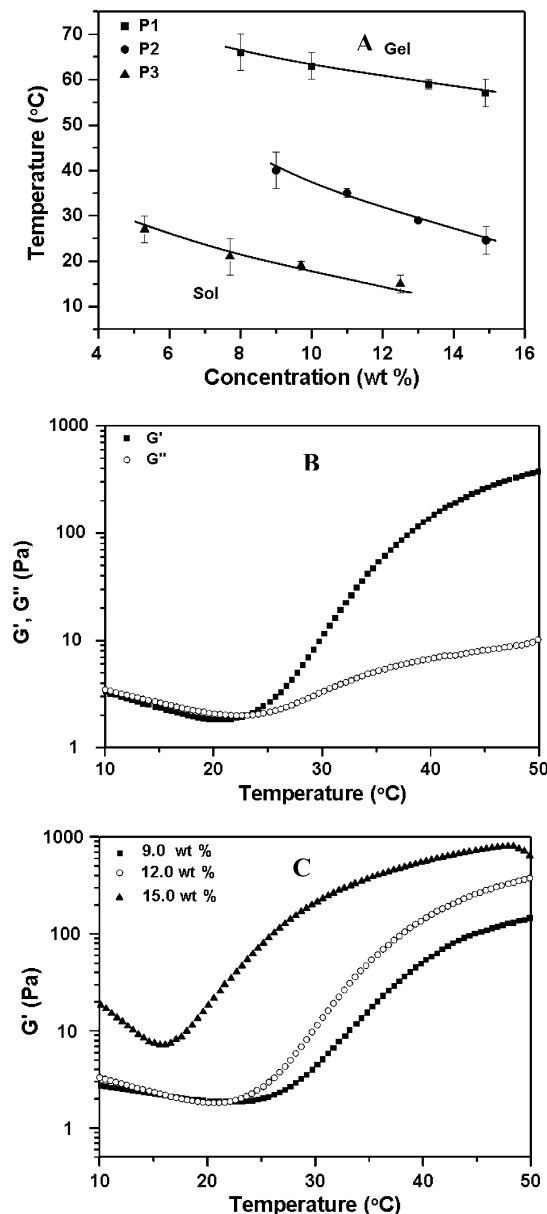


**Figure 3.** (A) Sol–gel phase diagrams of the block copolymer solutions (P1: PEG<sub>45</sub>-PPLG<sub>6</sub>; P2: PEG<sub>45</sub>-PPLG<sub>10</sub>; P3: PEG<sub>45</sub>-PPLG<sub>15</sub>). (B) Increases in storage modulus ( $G'$ ) and loss modulus ( $G''$ ) of PEG<sub>45</sub>-PPLG<sub>10</sub> PBS solution (12.0 wt %) during the sol–gel transition. (C) Storage modulus ( $G'$ ) as a function of temperature, indicating the effect of the concentration on the sol–gel transition of PEG<sub>45</sub>-PPLG<sub>10</sub> PBS solution.

the concentration of the copolymer solution resulted in an enhancement in modulus (Figure 3C) and a decrease in transition temperature. At body temperature, the moduli were 117, 346, and 1970 Pa for the systems with the concentrations of 9.0, 12.0, and 15.0 wt %, respectively.

DLS was further performed to study the micelle size and distribution of P2 aqueous solution under various temperatures (Figure S3A). The micelles with the average radius of 20 nm were measured in the low temperature range (10–20 °C). When the temperature was increased to 30 °C, micelles began to form aggregates with a broader size distribution. However, a unimodal size distribution was still observed. In contrast, as the temperature was further enhanced to above 40 °C, significant

increase in the aggregates size accompanying a broad distribution was observed, which may be caused by the partial dehydration of the PEG blocks and the formation of micelle aggregation.<sup>45</sup>

To gain insight into the phase transition mechanism at the molecular level, <sup>13</sup>C NMR spectral change of P2 aqueous solution (12.0 wt % in D<sub>2</sub>O) was studied as a function of temperature. We investigated the conformation change of the PEG block with changing temperature. At the sol state, the peak assigned to PEG at 69.5–71.5 ppm was sharp, which indicated a highly dynamic state of the block copolymers. As the temperature increased from 20 to 60 °C, the broadening of the PEG peak was noticeable, and a downfield shifting was also observed (Figure S3B), suggesting that the molecular motion of PEG was restricted. Such behavior can be attributed to the partial dehydration of PEG with increasing temperatures.<sup>46,47</sup>

It is reported that the temperature change may affect the secondary structure of the polypeptides in thermosensitive hydrogel systems, which is related to the sol–gel transition.<sup>25,44</sup> We studied the CD spectra of P2 aqueous solution as a function of temperature. A positive band at 195 nm and a negative Cotton band at 210–220 nm, which are two characteristic Cotton bands corresponding to  $\beta$ -sheet conformation, were observed (Figure S3C).<sup>48</sup> As the temperature increased from 10 to 60 °C, the negative band at 217 nm slightly increased in their magnitude, indicating an increase in  $\beta$ -sheet conformation of the polypeptide block. This fact suggests that the sol–gel transition of the P2 solution is basically an aggregation of the  $\beta$ -sheet structure, accompanying a partial strengthening of the  $\beta$ -sheet structure.<sup>44,49</sup>

Based on the above observations, the sol–gel transition of the copolymer solutions is proposed as follows. In the lower temperature range, the copolymers assemble into micelles in the aqueous solution, which are composed of PEG shells and PPLG cores when the concentration is higher than the critical micelle concentration. With increasing temperature, PEG blocks become partial dehydration and  $\beta$ -sheet structure of PPLG is partially strengthened, which induce the aggregation of micelles with a broader distribution. The aggregation of micelles makes the solvent lose flowability and leads to form a continuous network, resulting in the gel formation.<sup>46,50</sup>

In a biocompatibility study of PEG-PPLG hydrogels, mouse fibroblast L929 cells were incorporated in the gels and the cell-encapsulating hydrogel matrices were incubated in complete DMEM for 14 days. Cell viability as a function of culture time was determined by using a Live-Dead assay kit. The viable (stained green) and dead cells (stained red) were visualized by fluorescence microscopy. Initial cell death was observed on the first day, and it was significantly reduced after one week (Figure 4). In addition, the proliferation of cells was obvious up to 14 days. These results showed that the hydrogels exhibited good cytocompatibilities.

To investigate the feasibility of these block copolymers as biodegradable matrices, the *in vitro* and *in vivo* biodegradation of the polypeptide hydrogels was evaluated. *In vitro* enzymatic degradation study was carried out in Tris-HCl buffer solution containing 0.2 mg mL<sup>-1</sup> proteinase K. PEG<sub>45</sub>-PPLG<sub>10</sub> solutions in PBS (12.0 wt %) were first placed in 4 mL vials (diameter = 16 mm) and incubated at 37 °C for 10 min to form free-standing gels. The degradation medium with or without enzyme were added on the top of the gels. Over 90% mass loss was observed for the gels incubated in the medium with proteinase K compared to only 10% mass loss for the control

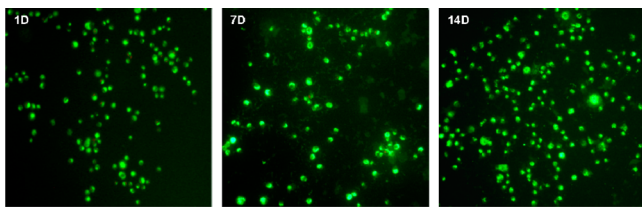


**Figure 4.** Live–dead assay showing L929 cells incorporated in the hydrogels after 1, 7, and 14 days in culture. Cells were stained with calcein-AM/PI and visualized using fluorescence microscopy. Green and red images indicated live and dead cells, respectively.

group after 13 days (Figure 5A). The result demonstrated that the enzymatic degradation of in situ formed hydrogels was driven by the surface erosion and the fast degradation of polypeptide chains.<sup>24,27</sup>

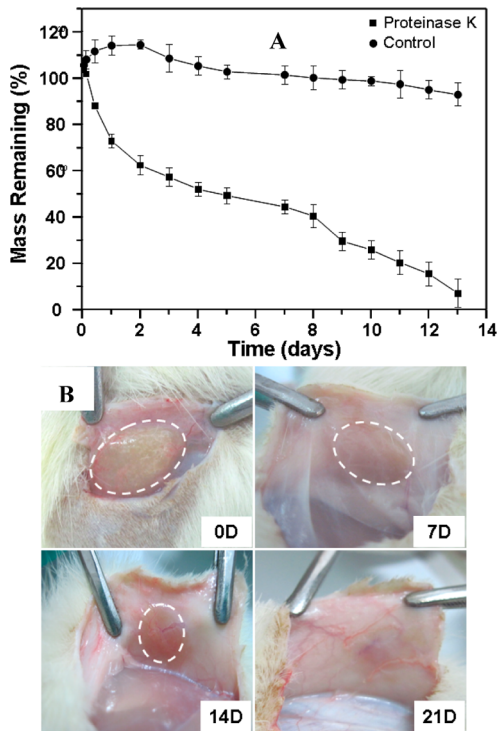


**Figure 5.** (A) In vitro mass loss profiles for the in situ formed hydrogels of PEG<sub>45</sub>-PPLG<sub>10</sub> (12.0 wt %) incubated in 0.05 M Tris-HCl buffer (pH 7.4) containing 0.2 mg mL<sup>-1</sup> proteinase K and in Tris-HCl buffer without proteinase K as control, respectively. (B) In vivo gel maintenance. The copolymer solutions in PBS (0.5 mL, 12.0 wt %) were subcutaneously injected into rats. Photos around the implants (marked as white-dotted curves) were taken 15 min (0 day), 7, 14, and 21 days after the injection.

In vivo gel formation and degradation were observed in SD rats. The copolymer solutions (12.0 wt %, 0.5 mL/rat) were injected into the subcutaneous layer of rats. At 15 min post-injection, hydrogels were observed in situ in the subcutaneous layer (Figure 5B). The integrity of the gels remained up to 15 days, while the overall size decreased gradually. At 3 weeks following injection, the gels were no longer detectable at the injection sites. Typical photographs are shown in Figure 5B.

The inflammatory response of the implanted gels was studied by H&E staining of the surrounding tissues at different intervals. At day 7 following injection of the gels, considerable

neutrophils were observed (Figure 6), indicating acute inflammatory reaction in the initial days after injection.

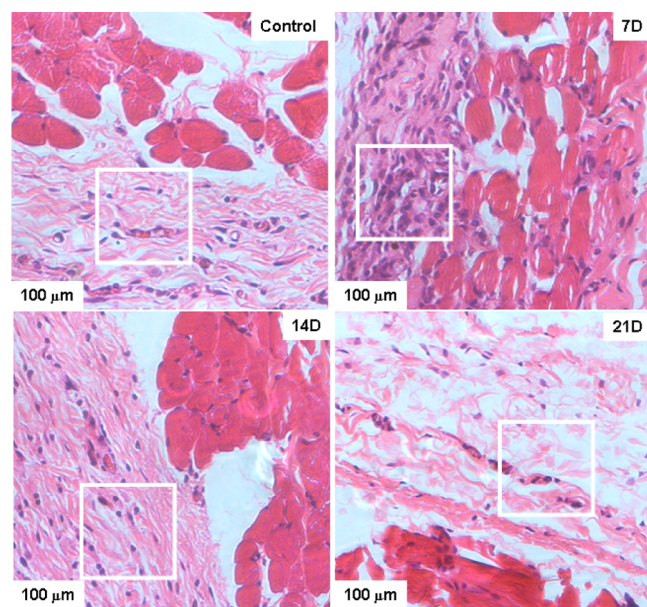
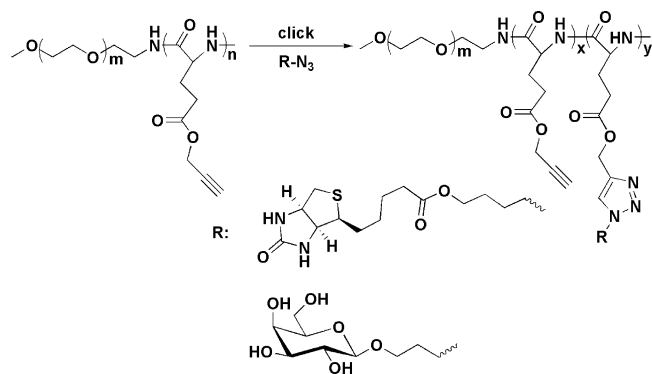


**Figure 6.** Tissue biocompatibility of the implant 7, 14, and 21 days after subcutaneous injection of PEG<sub>45</sub>-PPLG<sub>10</sub> gel. The normal subcutaneous tissue was taken as the blank control. H&E stained images around the implanted gel.

Notably, at two weeks postinjection, neutrophils were markedly reduced, and the critical inflammatory reaction was gradually replaced by a mild chronic inflammation. Furthermore, at 3 weeks postinjection, the gels completely disappeared and the histology of the tissue sample surrounding the injection site was almost restored to normal (control). Although acute inflammatory reaction was found surrounding the injection site, it was significantly reduced and eventually eliminated accompanying the degradation of the gels.<sup>51</sup> Hence, it suggested that the polypeptide hydrogels exhibited acceptable in vivo biocompatibility, which may be suitable for in vivo applications.

In addition, due to the presence of pendent alkynyl groups in the polypeptide block, various bioactive molecules can be easily introduced into the thermogelling PEG-polypeptide block copolymers. In this work, biotin and galactose were incorporated into PEG<sub>45</sub>-PPLG<sub>10</sub> via click chemistry, respectively (Scheme 2). Based on <sup>1</sup>H NMR spectra (Figure 7A),

**Scheme 2. Synthetic Routes of Biotin or Galactose Modified Poly(ethylene glycol)-block-poly( $\gamma$ -propargyl-L-glutamate)**



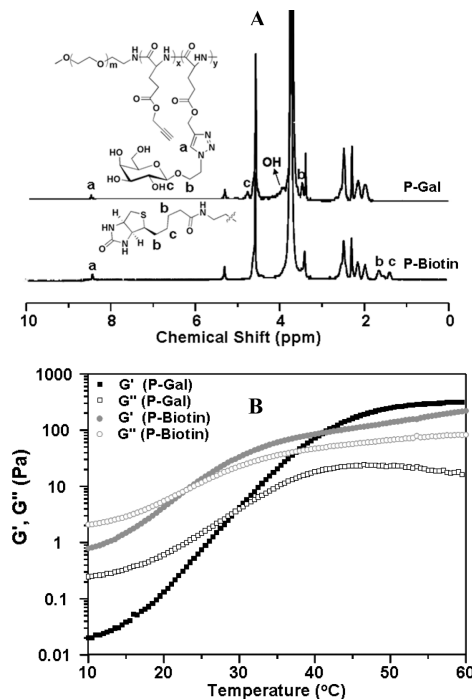


**Figure 7.** (A) <sup>1</sup>H NMR spectra of P-Gal and P-biotin in TFA-d. (B) Changes in the modulus of P-Gal and P-biotin PBS solution (12.0 wt %) as a function of temperature.

there were about 1.2–1.3 bioactive molecules per copolymer chain. After modification, biotin- and galactose-linked copolymers (denoted as P-Biotin and P-Gal) also displayed sol–gel transitions with increasing temperature, and their temperature-dependent modulus change was investigated by DMA, as shown in Figure 7B. Compared with the parent PEG-PPLG, P-Gal showed an enhanced phase transition temperature due to the increase in the hydrophilicity, while the critical gelation temperature (CGT) of P-biotin was slightly declined compared to the unmodified copolymer due to the relative hydrophobic nature of biotin.

We have investigated the level of residual copper salts by ICP-OES, and the results showed that the Cu contents were 0.05 and 0.04 wt % for galactose- and biotin-functionalized copolymers, respectively. In vitro cytotoxicities evaluated by MTT assay showed that L929 cells treated with the copolymers remained almost 100% viable at all concentrations up to 2.0 g L<sup>-1</sup>, indicating good biocompatibility of the block copolymers (Figure S4). Similar to the PEG-PPLG hydrogels, galactose-functionalized polypeptide hydrogels degraded completely within 3 weeks in vivo after subcutaneous injection into SD rats (Figure SSA). In addition, histological analysis indicated that a mild inflammatory reaction of surrounding tissues was observed, which was eliminated gradually accompanying with the degradation of the hydrogels (Figure SSB). The above study implied that the trace amount of the residual copper salts showed no obvious effect on the cytotoxicity, biodegradation, and biocompatibility of the modified copolymers.

The introduction of bioactive molecules may promote the interaction between cells and hydrogels. The hydrophilic galactose mostly emerged at the surface of hydrogels, could mediate the progress of cell adhesion. As shown in Figure 8, cell attachment on P-Gal gels was found to be significantly better than that on either P-biotin or unmodified gels. Although sugars are hydrophilic in nature, specific orientations of their

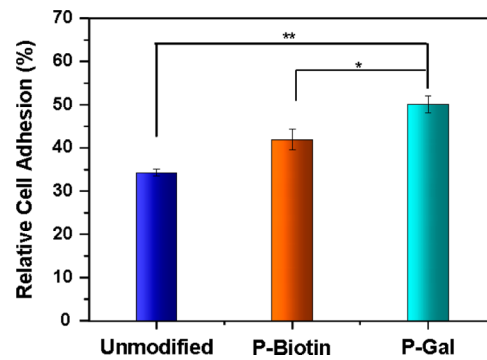


**Figure 8.** Adhesion of L929 cells on the hydrogels. Values and error bars represent the means of three independent experiments with triplicate samples and standard deviations with statistical significance (\* $p < 0.05$ , \*\* $p < 0.01$ ).

nonpolar –CH groups can create a hydrophobic patch, which may interact with a hydrophobic pocket at the receptor site on the protein.<sup>52</sup> FN plays a crucial role in mediating cell adhesion via integrin receptors, which widely exists in ECM. The exposed sugar units could adsorb FN in ECM, and FN further mediates the adhesion of cells. Biotin can also enhance cell affinity and promote cell adhesion through the interaction with its receptors on the cell surface. However, biotin molecules tended to assemble into the hydrophobic core of the amphiphilic aggregates in PBS, and the gel surface was rich of PEG segments, leading to restriction of cell adhesion. This result confirmed that the high cell adhesion on the P-Gal gels was attributed to the mediation of FN.

## CONCLUSIONS

Thermosensitive in situ forming hydrogels based on PEG and poly(L-glutamate) were prepared by ROP of PLG NCA in the presence of amino-terminated mPEG. The concentrated solutions of the resulting copolymers underwent a sol–gel phase transition as a function of temperature. Mouse fibroblast L929 cells encapsulated in the hydrogel matrices showed high viability. The mass loss of the hydrogel in vitro was accelerated in the presence of proteinase K, and in situ formed gels in the subcutaneous layer of rats showed a duration of 3 weeks. H&E staining study suggested acceptable in vivo biocompatibility of the PEG-polypeptide hydrogels.

The resulting copolymers, which contained alkynyl groups, could be functionalized with various bioactive molecules, for example, biotin and galactose, via click chemistry. The biofunctionalized copolymers retained sol–gel phase transition properties near body temperature. In contrast to biotin, the hydrophilic galactose promoted cell adhesion on the hydrogel surface. Our present work provides an interesting platform on the fabrication of biofunctionalized in situ forming hydrogels, which could facilitate the mediation of the biofunction of the materials and regulating the cell–material interactions.

## ASSOCIATED CONTENT

### Supporting Information

Deconvolution of the FTIR spectra of PEG<sub>45</sub>-PPLG<sub>10</sub> aqueous solution (Figure S1), TEM image of PEG<sub>45</sub>-PPLG<sub>10</sub> micelles (Figure S2A), the excitation spectra of pyrene in PEG<sub>45</sub>-PPLG<sub>10</sub> aqueous solutions (Figure S2B), the intensity ratio of  $I_{336}/I_{332}$  as a function of concentration of the resulted copolymers (Figure S2C), <sup>13</sup>C NMR spectra of 12.0 wt %

PEG<sub>45</sub>-PPLG<sub>10</sub> solution in D<sub>2</sub>O as a function of temperature (Figure S3A), distribution of hydrodynamic radius ( $R_h$ ) of micelles of PEG<sub>45</sub>-PPLG<sub>10</sub> (P2) as a function of temperature in water (1.0 wt %; Figure S3B), circular dichroism spectra of 0.05 wt % PEG<sub>45</sub>-PPLG<sub>10</sub> aqueous solution as a function of temperature (Figure S3C), in vitro cytotoxicities of the modified block copolymers (Figure S4), in vivo gel maintenance and biocompatibility of the modified copolymers (Figure S5). This material is available free of charge via the Internet at <http://pubs.acs.org>.

## AUTHOR INFORMATION

### Corresponding Author

\*E-mail: xschen@ciac.jl.cn.

### Notes

The authors declare no competing financial interest.

## ACKNOWLEDGMENTS

The authors are grateful for the financial support from the National Natural Science Foundation of China (Projects 51003103, 21174142, 50973108, 51233004, and 51021003), the Ministry of Science and Technology of China (International Cooperation and Communication Program 2011DFR51090), and the Scientific Development Program of Jilin Province (201101082, 20110332).

## REFERENCES

- (1) Chang, G. T.; Ci, T. Y.; Yu, L.; Ding, J. D. *J. Controlled Release* **2011**, *156*, 21–27.
- (2) He, C.; Zhuang, X.; Tang, Z.; Tian, H.; Chen, X. *Adv. Healthcare Mater.* **2012**, *1*, 48–78.
- (3) Jeong, B.; Bae, Y. H.; Lee, D. S.; Kim, S. W. *Nature* **1997**, *388*, 860–862.
- (4) Choi, B. G.; Park, M. H.; Cho, S. H.; Joo, M. K.; Oh, H. J.; Kim, E. H.; Park, K.; Han, D. K.; Jeong, B. *Biomaterials* **2010**, *31*, 9266–9272.
- (5) Yun, E. J.; Yon, B.; Joo, M. K.; Jeong, B. *Biomacromolecules* **2012**, *13*, 1106–1111.
- (6) Geisler, I. M.; Schneider, J. P. *Adv. Funct. Mater.* **2012**, *22*, 529–537.
- (7) Balakrishnan, B.; Banerjee, R. *Chem. Rev.* **2011**, *111*, 4453–4474.
- (8) Ibusuki, S.; Fujii, Y.; Iwamoto, Y.; Matsuda, T. *Tissue Eng.* **2003**, *9*, 371–384.
- (9) Dang, J. M.; Sun, D. D. N.; Shin-Ya, Y.; Sieber, A. N.; Kostuik, J. P.; Leong, K. W. *Biomaterials* **2006**, *27*, 406–418.
- (10) Freudenberg, U.; Hermann, A.; Welzel, P. B.; Stirl, K.; Schwarz, S. C.; Grimmer, M.; Zieris, A.; Panyanuwat, W.; Zschoche, S.; Meinhold, D.; Storch, A.; Werner, C. *Biomaterials* **2009**, *30*, 5049–5060.
- (11) He, C. L.; Kim, S. W.; Lee, D. S. *J. Controlled Release* **2008**, *127*, 189–207.
- (12) Yu, L.; Ding, J. D. *Chem. Soc. Rev.* **2008**, *37*, 1473–1481.
- (13) Huynh, C. T.; Nguyen, M. K.; Lee, D. S. *Macromolecules* **2011**, *44*, 6629–6636.
- (14) Park, M. H.; Joo, M. K.; Choi, B. G.; Jeong, B. *Acc. Chem. Res.* **2012**, *45*, 424–433.
- (15) Moon, H. J.; Ko, D. Y.; Park, M. H.; Joo, M. K.; Jeong, B. *Chem. Soc. Rev.* **2012**, *41*, 4860–4883.
- (16) Hiemstra, C.; Zhou, W.; Zhong, Z. Y.; Wouters, M.; Feijen, J. *J. Am. Chem. Soc.* **2007**, *129*, 9918–9926.
- (17) Lee, J.; Bae, Y. H.; Sohn, Y. S.; Jeong, B. *Biomacromolecules* **2006**, *7*, 1729–1734.
- (18) Yu, L.; Zhang, H.; Ding, J. D. *Angew. Chem., Int. Ed.* **2006**, *45*, 2232–2235.
- (19) Yu, L.; Zhang, Z.; Ding, J. D. *Biomacromolecules* **2011**, *12*, 1290–1297.
- (20) Gong, C. Y.; Shi, S. A.; Wu, L.; Gou, M. L.; Yin, Q. Q.; Guo, Q. F.; Dong, P. W.; Zhang, F.; Luo, F.; Zhao, X.; Wei, Y. Q.; Qian, Z. Y. *Acta Biomater.* **2009**, *5*, 3358–3370.
- (21) Shim, W. S.; Kim, S. W.; Lee, D. S. *Biomacromolecules* **2006**, *7*, 1935–1941.
- (22) Loh, X. J.; Goh, S. H.; Li, J. *Biomacromolecules* **2007**, *8*, 585–593.
- (23) Nguyen, M. K.; Park, D. K.; Lee, D. S. *Biomacromolecules* **2009**, *10*, 728–731.
- (24) Moon, H. J.; Choi, B. G.; Park, M. H.; Joo, M. K.; Jeong, B. *Biomacromolecules* **2011**, *12*, 1234–1242.
- (25) Park, S. H.; Choi, B. G.; Moon, H. J.; Cho, S. H.; Jeong, B. *Soft Matter* **2011**, *7*, 6515–6521.
- (26) Jeong, Y.; Joo, M. K.; Bahk, K. H.; Choi, Y. Y.; Kim, H. T.; Kim, W. K.; Lee, H. J.; Sohn, Y. S.; Jeong, B. *J. Controlled Release* **2009**, *137*, 25–30.
- (27) Cheng, Y. L.; He, C. L.; Xiao, C. S.; Ding, J. X.; Zhuang, X. L.; Huang, Y. B.; Chen, X. S. *Biomacromolecules* **2012**, *13*, 2053–2059.
- (28) Muthukrishnan, S.; Nitschke, M.; Gramm, S.; Ozyurek, Z.; Voit, B.; Werner, C.; Muller, A. H. E. *Macromol. Biosci.* **2006**, *6*, 658–666.
- (29) Chen, X. M.; Dordick, J. S.; Rethwisch, D. G. *Macromolecules* **1995**, *28*, 6014–6019.
- (30) Bowman, B. B.; Rosenberg, I. H. *J. Nutr.* **1987**, *117*, 2121–2126.
- (31) Na, K.; Lee, T. B.; Park, K. H.; Shin, E. K.; Lee, Y. B.; Cho, H. K. *Eur. J. Pharm. Sci.* **2003**, *18*, 165–173.
- (32) Cannizzaro, S. M.; Padera, R. F.; Langer, R.; Rogers, R. A.; Black, F. E.; Davies, M. C.; Tendler, S. J. B.; Shakesheff, K. M. *Biotechnol. Bioeng.* **1998**, *58*, 529–535.
- (33) Sakahara, H.; Saga, T. *Adv. Drug Delivery Rev.* **1999**, *37*, 89–101.
- (34) Ding, J. X.; Shi, F. H.; Xiao, C. S.; Lin, L.; Chen, L.; He, C. L.; Zhuang, X. L.; Chen, X. S. *Polym. Chem.* **2011**, *2*, 2857–2864.
- (35) Xiao, C. S.; Zhao, C. W.; He, P.; Tang, Z. H.; Chen, X. S.; Jing, X. B. *Macromol. Rapid Commun.* **2010**, *31*, 991–997.
- (36) Cheng, Y.; He, C.; Xiao, C.; Ding, J.; Zhuang, X.; Chen, X. *Polym. Chem.* **2011**, *2*, 2627–2634.
- (37) Heo, D. N.; Yang, D. H.; Moon, H. J.; Lee, J. B.; Bae, M. S.; Lee, S. C.; Lee, W. J.; Sun, I. C.; Kwon, I. K. *Biomaterials* **2012**, *33*, 856–866.
- (38) Haris, P. I.; Chapman, D. *Biopolymers* **1995**, *37*, 251–263.
- (39) Choi, Y. Y.; Jang, J. H.; Park, M. H.; Choi, B. G.; Chi, B.; Jeong, B. *J. Mater. Chem.* **2010**, *20*, 3416–3421.
- (40) Baginska, K.; Makowska, J.; Wiczek, W.; Kasprzykowski, F.; Chmurzynski, L. *J. Pept. Sci.* **2008**, *14*, 283–289.
- (41) Ding, J. X.; Xiao, C. S.; Zhao, L.; Cheng, Y. L.; Ma, L. L.; Tang, Z. H.; Zhuang, X. L.; Chen, X. S. *J. Polym. Sci., Part A: Polym. Chem.* **2011**, *49*, 2665–2676.
- (42) Wang, W.; Ding, J. X.; Xiao, C. S.; Tang, Z. H.; Li, D.; Chen, J.; Zhuang, X. L.; Chen, X. S. *Biomacromolecules* **2011**, *12*, 2466–2474.
- (43) Tanodekaew, S.; Godward, J.; Heatley, F.; Booth, C. *Macromol. Chem. Phys.* **1997**, *198*, 3385–3395.
- (44) Kim, E. H.; Joo, M. K.; Bahk, K. H.; Park, M. H.; Chi, B.; Lee, Y. M.; Jeong, B. *Biomacromolecules* **2009**, *10*, 2476–2481.
- (45) Yu, L.; Zhang, Z.; Zhang, H.; Ding, J. D. *Biomacromolecules* **2009**, *10*, 1547–1553.
- (46) Yu, L.; Chang, G. T.; Zhang, H.; Ding, J. D. *J. Polym. Sci., Part A: Polym. Chem.* **2007**, *45*, 1122–1133.
- (47) Wang, Y. C.; Xia, H.; Yang, X. Z.; Wang, J. *J. Polym. Sci., Part A: Polym. Chem.* **2009**, *47*, 6168–6179.
- (48) Nuhn, H.; Klok, H. A. *Biomacromolecules* **2008**, *9*, 2755–2763.
- (49) Oh, H. J.; Joo, M. K.; Sohn, Y. S.; Jeong, B. *Macromolecules* **2008**, *41*, 8204–8209.
- (50) Kim, S. Y.; Kim, H. J.; Lee, K. E.; Han, S. S.; Sohn, Y. S.; Jeong, B. *Macromolecules* **2007**, *40*, 5519–5525.
- (51) Yu, L.; Zhang, Z.; Zhang, H. A.; Ding, J. D. *Biomacromolecules* **2010**, *11*, 2169–2178.
- (52) Rao, V. S. R.; Lam, K.; Qasba, P. K. *Int. J. Biol. Macromol.* **1998**, *23*, 295–307.